

### **3. SYNTHESIS PROCEDURE AND CHARACTERIZATIONS**

Pyrochlore ceramic compounds are synthesized in various ways for advanced potential multifunctional applications. There are numerous synthesis procedures to obtain ceramic oxides including both wet and dry chemical methods. The wet chemical method for ceramics comprises sol-gel, co-precipitation etc [1-6] whereas dry chemical method includes a well known solid state reaction method or ceramic method [7].

The characterization of ceramic materials is an essential aspect for understanding their properties for its potential applications. This chapter offers the discussion of the well known solid state reaction method for the synthesis of pyrochlore ceramic materials. Various characteristics for applications of synthesized ceramics are also discussed in this chapter. Since many decades, ceramic materials were produced with traditional techniques that did not allow synthesis control and desirable textural properties. The technique employed in this work allows the production of solids with controllable size and shape. These materials can be produced with well-defined structure and morphology.

#### **3.1 Solid State Reaction Mechanism**

Different inorganic solids can be synthesized through the reaction of a solid with another solid (“solid/solid” reaction), a liquid (melt) or a gas (“solid/gas” reaction) at high temperature. Also, solids can turn into melt or gaseous intermediates through the ongoing reaction. Solid/solid reaction or ceramic method has been widely applied for the production of oxides for a long time. The combination of solid and gaseous reactants gives a better contact between them in comparison to that between just two solids [8-11].

The ceramic method is the oldest method for the synthesis of solid-state materials [12, 13]. High temperatures are required for solids to react with each other. The advantages of this method include low cost of production, available precursors, and simplicity of the processes. The shortcomings include formation of undesirable phases, non-homogeneous distribution of dopants, and a difficulty in monitoring the reaction progress. High temperature in this method requires the application of chemically inert materials such as containers (platinum, silica, stabilized zirconia, and alumina).

The reaction goes through the formation of product nuclei at the interface of the solids. The growth of the product layer slows down the counter diffusion of ions from the reacting solids to each other and decreases the rate of the reaction. Only very high temperatures provide enough energy for ions to diffuse through. To maximize the reaction rates, the starting precursors need to be well ground to increase surface areas and contact between particles.

The solid-state reaction depends on the reactivity of the starting precursors. The final oxide products can be produced by the oxidation of precursors by oxygen from the air or by the reaction during the decomposition of the precursor compounds. The pyrochlore structure, of general formula  $A_2B_2O_7$  can be produced by the solid-state reaction of bismuth oxide ( $Bi_2O_3$ ), vanadium pentoxide ( $V_2O_5$ ) with different doping concentration of copper oxide (CuO) and magnesium oxide (MgO). These metal oxides reacts to form intermediate layer of the  $(BiV)_{1.5}(Cu_{1-x}Mg_x)O_7$  ( $x = 0, 0.2, 0.4, 0.5, 0.6, 0.8$  and 1) phase[3]. This phase allows the migration of cations from the CuO and MgO within the pyrochlore phase [14]. The same approach can be used for the synthesis of other mixed metal oxides; however, the reactions between two solids

may not occur due to unfavorable thermodynamic conditions (slow reaction rates, slow diffusion, or very high temperatures).

### **3.2 Synthesis of $(\text{Bi}_{1.5}\text{Mg}_x\text{Cu}_{1-x}\text{V}_{1.5})\text{O}_7$ ceramics**

Rare earth substituted BMCV-ceramic compounds was synthesized by well-known solid state reaction method. The starting materials  $\text{Bi}_2\text{O}_3$ ,  $\text{V}_2\text{O}_5$ ,  $\text{MgO}$ , and  $\text{CuO}$  (all Aldrich make 99.99%) were weighed in stoichiometric proportions. The weighed chemicals were mixed by grinding homogeneously. The grounded samples were calcined at 923 K for 4 h to remove impurities like carbon present, using temperature controlled programmable muffle furnace. At 923 K, the calcined powder was again grounded and then heated for 4 h to initiate the formation of single phase pyrochlore structure. Finally, the calcined powders were pressed isostatically into circular pellets at pressure of 100 MPa using a hydraulic press and sintered at 963 K for 4 h in air to obtain final product. Fig. 3.1 shows the synthesis flow chart of the ceramics synthesized using solid state reaction method.

In order to characterize the structure of ceramics, the pellets were crushed and powdered for XRD and SEM studies. However, the electrical measurements were performed using the pellets coated with silver paste on both the sides. The silver coat acts as a electrodes on the surface of ceramics.



$$n\lambda = 2d\sin\theta \dots\dots\dots (3.1)$$

Where  $d$  is interplanar spacing given as

$$d = \frac{n\lambda}{2\sin\theta} \dots\dots\dots (3.2)$$

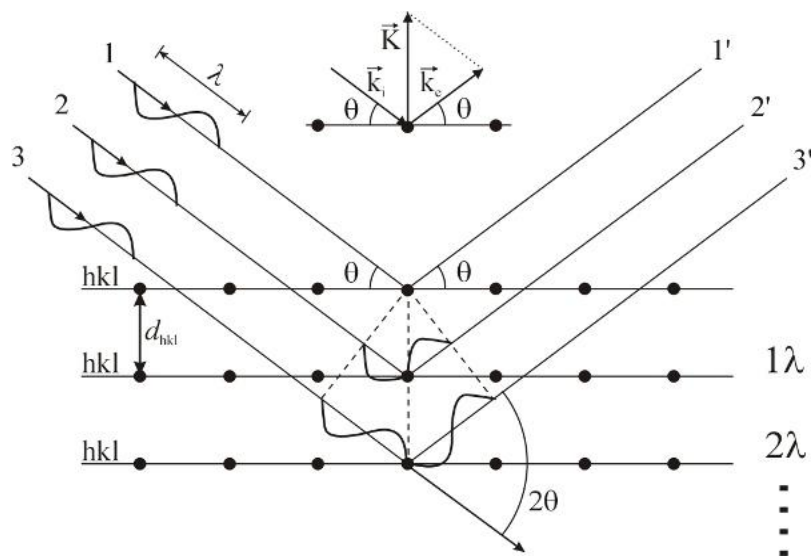


**Fig. 3.2 Basic principle involved in diffraction of X-ray beam from assembly of lattice-atoms**

The powder profile of a substance, even without further interpretation, can be used for identification of materials. The following information can be obtained from their X-Ray powder diffractogram:

- I. Quality and confirmation of the prepared samples
- II. The interplanar spacing  $d$  of the reflections
- III. The intensities of the reflections, and
- IV. The unit cell dimensions and lattice type.

In the present case, calcined powders were characterized with respect to phase identification, phase quantity measurement, crystallite size determination and lattice parameter measurement, etc., all by using Philips, PANalytical PRO Diffractometer

using  $\text{CuK}\alpha$ -radiation with Ni-filter ( $\lambda=1.54056\text{\AA}$ ) at room temperature. For quantitative estimation of phases, calcined powders were uniformly mixed and the resulting mixture was analyzed using a step size of  $2^\circ/\text{min}$ . The relative weight fractions were quantified from the ratio of peak areas. The phases giving maximum peak area at a particular temperature were considered as 100% formation of those phases at that temperature. Considering that area as 100%, the relative percentages of the respective phases were calculated. On the basis of full width half maxima of highest intensity peak from XRD pattern, crystallite size of the phases were estimated using the Scherrer equation, as [18, 19];

$$t = \frac{0.89\lambda}{B\cos\theta} \dots\dots\dots 3.3$$

where t-linear particle size,  $k\lambda = 0.89$  (constant),  $\theta$  = peak position and B = full width half maximum peak. The x-ray density ( $\rho$ ) of the specimen was calculated by using

$$\rho = \frac{\sum \frac{A}{N}}{V} \dots\dots\dots (3.4)$$

A is the atomic weight of the sample, N is the Avogadro's number and V is Volume of the unit cell given as

$$V_{\text{mon}} = a * b * c * \sin(\beta) \dots\dots\dots (3.5)$$

Where a, b and c are the lattice parameters and given as

$V_{\text{mon}}$  unit cell volume ( $\text{\AA}^3$ ),

**a** vector(one of the sides of the a rectangular base) ( $\text{\AA}$ )

**b** vector(the other side of the rectangular base) ( $\text{\AA}$ )

**c** vector(the edge of the parallelogram side plane) ( $\text{\AA}$ )

$$\frac{1}{d^2} = \left( \frac{h^2}{a^2} + \frac{k^2 \sin^2(\beta)}{b^2} + \frac{l^2}{c^2} - \frac{2hlc \cos(\beta)}{ac} \right) \dots \dots \dots (3.6)$$

Where h, k, l are the Miller indices. For monoclinic crystal  $\alpha = \gamma = 90^\circ$  but  $\beta \neq 90^\circ$

### 3.3.3 Scanning Electron Microscope

The scanning electron microscopy (SEM) is a useful technique to study the morphology, topography and composition of the materials with much higher resolution. When a beam of highly energetic electrons strikes the sample, the secondary electrons, x-rays and back-scattered electrons are ejected from the sample [20]. These electrons are then collected by the detector and convert into signal that displays on a screen. In the present study, the SEM micrograph was taken on the fractured surface of the sample using scanning electron microscope (SEM: JSM-840 scanning microscope JEOL). As the samples are non-conducting, a thin layer of gold is coated using a sputter coater.

For measurement of the grain size, some lines of known length were drawn on the micrograph. The number of grains cut by the lines was counted. Then the average grain size was calculated by the standard line intercept method given by equation [21]

$$Grain - size = \frac{1.56C}{MN} \dots \dots \dots (3.7)$$

Where C= length of the Scale, M= Magnification and N=No of Intercepts.

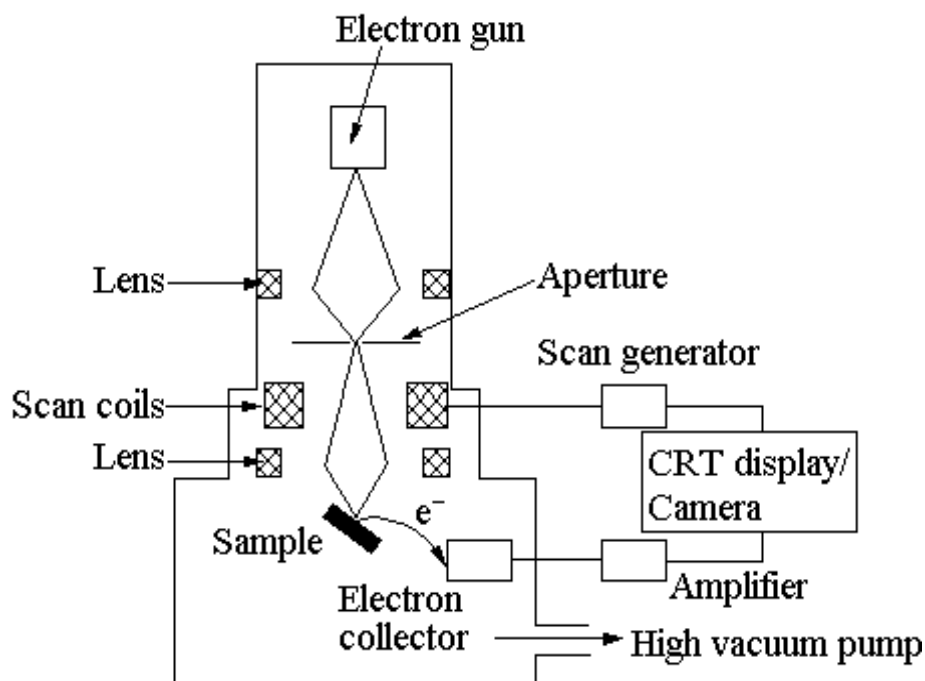


**Fig. 3.3 Schematic diagram of Scanning Electronic Microscopy**

### 3.3.4 Energy-dispersive spectrometer

Energy-dispersive spectrometer (EDS) is a technique used for quantitative analysis for determination of the concentrations of the elements present in the synthesized pyrochlore compounds. EDS makes use of the X-ray spectrum emitted by a solid sample bombarded with a focused beam of electrons to obtain a localized chemical analysis. All elements from atomic number 4 (Be) to 92 (U) can be detected in principle, though qualitative analysis involves the identification of the lines in the spectrum and is fairly straightforward owing to the simplicity of X-ray spectra. Energy-dispersive spectrometers (EDS) employ pulse height analysis, a detector giving output pulses proportional in height to the X-ray photon energy is used in conjunction with a pulse height analyzer.

A solid state detector is used because of its better energy resolution. Incident X-ray photons cause ionization in the detector, producing an electrical charge, which

is amplified by a sensitive preamplifier located close to the detector. Both detector and preamplifier are cooled with liquid nitrogen to minimize electronic noise. Si (Li) or Si drift detectors (SDD) are commonly in use. The ED spectrum is displayed in digitized form with the x-axis representing X-ray energy (usually in channels 10 or 20 eV wide) and the y-axis representing the number of counts per channel. An X-ray line (consisting of effectively mono-energetic photons) is broadened by the response of the system, producing a Gaussian profile. Energy resolution is defined as the full width of the peak at half maximum height (FWHM).

Conventionally, this is specified for the Mn K $\alpha$  peak at 5.89 keV. For Si (Li) and SDD detectors, values of 130-150eV are typical (Ge detectors can achieve 115eV). The resolution of an EDS is good enough to separate the K lines of neighboring elements [22].

### **3.4 Electrical Studies**

#### **3.4.1 DC Resistivity**

DC resistivity is measured using two probe method. A standard experimental unit for this measurement was employed. Thin polished and silver coated pellet (10mm diameter and 2mm thickness) was placed in between two spring-loaded foils of the electrode. A constant voltage source (DC voltage=10V) was used to apply potential across the pellet. The temperature was measured with a chromel alumel thermocouple, a tip of which was maintained in close proximity to the sample for maximum accuracy. The value of current was measured using nano-ammeter during cooling, in the temperature range from 313K to 773K at the interval of 10K and the resistance was calculated. Resistivity ( $\rho$ ) of all samples was estimated using the relation [23],

$$\rho = R \times \left( \frac{A}{d} \right) \dots\dots\dots (3.8)$$

Where R= resistance, A= area of the pellet ( $\pi r^2$ ) and d=thickness of the sample. Since, the Van der Paw analysis is based on four probe technique for irregular shaped samples, the objective of our two probe dc resistivity measurement is to determine the resistance by applying constant dc voltage (here, 10V) and measure the current.

### **3.4.3 Impedance study**

The complex impedance spectroscopy is a powerful tool to investigate the electrical properties of the complex pyrochlore oxides [24]. The main advantages of the technique are -

- i) it involves relatively simple electrical measurements that can readily be automated,
- ii) the measurements can be implemented by using arbitrary electrodes,
- iii) the results can be often correlated with the properties such as composition, microstructure, defects, dielectric properties, chemical reaction etc. of the sample and
- iv) the resistance of the grain boundaries and that of grains can be easily separated in most of the polycrystalline samples [25].

AC measurements are often made with a Wheatstone bridge type of apparatus (Impedance analyzer or LCR-Q meter) in which the resistance  $R$  and capacitance  $C$  of the sample are measured and balanced against variable resistors and capacitors. The impedance  $|Z|$  and the phase difference ( $\theta$ ) between the voltage and current are measured as a function of frequency ( $f$ ) for the given sample and the technique is called impedance spectroscopy.

Analysis of the data is carried out by plotting the imaginary part of the impedance  $Z''=|Z| \cos\theta$  against the real part  $Z'=|Z|\sin\theta$  on a complex plane called

the impedance plot. An impedance plot with linear scale is used to analyze the equivalent circuit as follows:

Impedance plot of a pure resistor is a point on real axis and that of pure capacitor is a straight line coinciding with the imaginary axis. The impedance of a parallel RC combination is expressed by the following relation [26],

$$Z^* = Z' - jZ'' = \frac{R}{1+j\omega RC} \dots\dots\dots (3.9)$$

### 3.4.4 Dielectric Measurement Set-up

Dielectric characteristics of ceramic materials are of prime importance as the field of solid-state electronics continues to expand rapidly. The principal applications for ceramic dielectrics are as capacitive elements in electronic circuits and as electrical insulation. For these applications, the properties of most concern are the dielectric constant, dielectric loss factor and dielectric strength. New devices and new applications are continually increasing the frequency range and range of environmental conditions, particularly temperature, that are of practical interest. In an ideal capacitor, the electric charge adjusts itself instantaneously to any change in voltage. In practice, however, there is inertia to charge movement that shows up as a relaxation time for charge transport. It is a measure of the time lag of the system.

The dielectric permittivity is measured as function of temperature in the range 623K to 303K during natural cooling furnace. The dielectric constant is calculated by using the formula [27].

$$\epsilon = \frac{C \times t}{\epsilon_o \times A} \dots\dots\dots (3.10)$$

Where A is Area of cross-section of the sample, t is thickness of the sample and  $\epsilon_o = 8.854 \times 10^{-12}$  F/m.

## **References**

1. S. T. Neirman, *J Mater. Sci.* 3973-3980, 23, (1988).
2. S. Kazaoui, J. Ravez, *J Mater. Sci.*, 1211-1216, 28, (1993).
3. P. W. Rehrig, S.E. Park, S. T. McKinstry, G. L. Missing, B. Jones, T. R. Shrout, *J. Appl. Phys*, 1657-1661, 86[3], (1999).
4. M. Veith, S. Mathur, N. Lecerf, V.Huch, T. Decker, *J Sol-Gel Sci.Tech.* 145-158, 15 (2000).
5. P. S. Dobal, A. Dixit, R. S. Katiyar, Z. Yu, R. Guo, A. S Bhalla, *J. Appl. Phys*, 8085-8089, 9, (2001).
6. Z Jiwei, Y. Xi, S. Bo, Z. Liangying, H. Chen, *J Electro Ceram*, 157-161, 11, (2003).
7. F. Moura, A. Z. Simoes, B. D. Stojanovic, M. A. Zaghete, E. Longo, J. A. Varela, *J Alloys Compd.*, 129-134, 462, (2008).
8. W. D. Swallo and A. K. Jordon, *Proc. Brit. Ceram. Sec.*, 45-50, 2 (1964).
9. J. E. Burke, “*Kinetics of High Temperature Processes*” New York, (1959).
10. C. Z. Wagner, *Phys. Chem.*, 309-313, B-34, (1936).
11. C .N. R. Rao, B. Raveau “*Transition Metal Oxides Structure, Properties and Synthesis of Ceramic Oxides*”, WILEY-VCH, New York, (2002).
12. M.N. Rahaman, *Sintering of Ceramics*, FL: CRC Press, Taylor and Francis Group, Boca Raton, (2008).
13. S.J. Kang L, *Sintering-densification, grain growth and microstructure*, Elsevier Amsterdam, (2005).
14. J E.D. Politova, E.A. Fortalnova, G.M. Kaleva, M.G. Safronenko, and N.U. Venskovsk., *Bulletin of the Russian Academy of Sciences: Phys*, 1069–1072, 74, (2010).
15. B D Cullity “*Elements of X – ray diffraction*” Addison Wesley pub. Co. Inc. Massachusetts, (1956).
16. M J Burger, “*X –ray Crystallography*”, Wiley, New York, (1953).
17. A N Raransky, Ja, M. Struk, I. M. Fodchuk and N D Raranskay, *Proc. SPIE – Int, Soc.Opt.Eng.USA*, 2108, 320, (1993).
18. B. F. Levine, *Phys.* 2591, B 87, (1975).
19. W L Bragg, *The crystalline state*, Macmillan, New York, (1993).

20. K. K. Bharathi, N. R. Kalidindi, C. V. Ramana, *J Appl Phys.*, 083529-083533, 108, (2010).
21. A. Mark. McCormick, B. E. Slamovich, *J. Am. Ceram. Soc.*, 442–44, 83[2], (2000).
22. J.C.Russ, *Fundamentals of Energy Dispersive X-ray Analysis*, Butter worths, London, (1984).
23. J. R. Macdonald, “*Impedance Spectroscopy Emphasizing Solid materials and Systems*”, John Wiley and Sons, New York, (1987).
24. Wieczorek. W, Plochanski. J, J. Przulski, *Solid State Ionics*, 28–30, 79, (1988).
25. E. A. Atekwana, E. A. Atekwana, R. S. Rowe, D. D. Werkema Jr. F. D. Legall, *J. Appl. Geophys.* 281– 294, 56 (2004).
26. R.S. Vemuri, K. Kamala Bharathi, S.K. Gullapalli, C.V. Ramana, *Appl Mater.*, 2623–2628, 2, (2010).
27. S. Ma, F. Liao, S. Xin Li, M. Xu, J. Li, S. Zhang, S. Chen, R. Huang, S. Gao., *J Mater Chem.*, 3096-3102, 13, (2003).